Gertz Likhtenshtein

WILEY-VCH

Solar Energy Conversion

Chemical Aspects

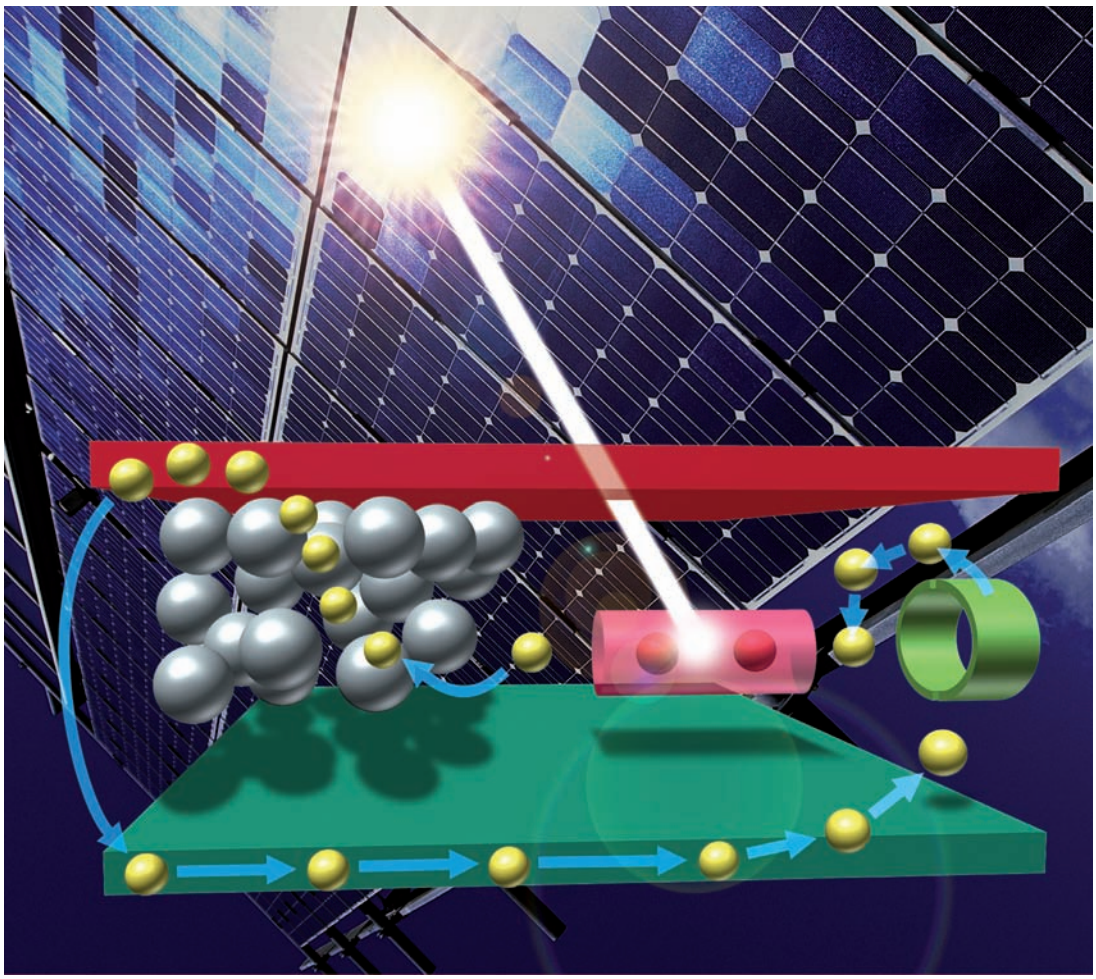

Gertz Likhtenshtein

Solar Energy Conversion

Related Titles

Strehmel, B., Strehmel, V., Malpert, J. H.

Applied and Industrial Photochemistry

2012

ISBN: 978-3-527-32668-6

Scheer, R., Schock, H.-W.

Chalcogenide Photovoltaics

Physics, Technologies, and Thin Film Devices

2011

ISBN: 978-3-527-31459-1

Alkire, R. C., Kolb, D. M., Lipkowski, J., Ross, P. (Eds.)

Photoelectrochemical Materials and Energy Conversion Processes

2010

ISBN: 978-3-527-32859-8

Würfel, P.

Physics of Solar Cells

From Basic Principles to Advanced Concepts

2009

ISBN: 978-3-527-40857-3

Pagliaro, M., Palmisano, G., Ciriminna, R.

Flexible Solar Cells

2008

ISBN: 978-3-527-32375-3

De Vos, A.

Thermodynamics of Solar Energy Conversion

2008

ISBN: 978-3-527-40841-2

Brabec, C., Scherf, U., Dyakonov, V. (Eds.)

Organic Photovoltaics

Materials, Device Physics, and Manufacturing Technologies

2008

ISBN: 978-3-527-31675-5

Gertz Likhtenshtein

Solar Energy Conversion

Chemical Aspects

WILEY-VCH Verlag GmbH & Co. KGaA

The Author

Prof. Gertz Likhtenshtein
Department of Chemistry
Ben Gurion University
P.O. Box 653
84105 Beer-Sheva
Israel

Library of Congress Card No.: applied for

British Library Cataloguing-in-Publication Data
A catalogue record for this book is available from the British Library.

Bibliographic information published by the Deutsche Nationalbibliothek
The Deutsche Nationalbibliothek lists this publication in the Deutsche Nationalbibliografie; detailed bibliographic data are available on the Internet at http://dnb.d-nb.de.

Composition Thomson Digital, Noida, India
Printing and Binding Markono Print Media Pte Ltd, Singapore
Cover Design Schulz Grafik-Design, Fußgönheim

Printed in Singapore
Printed on acid-free paper

Print ISBN: 978-3-527-32874-1

Contents

Preface

World energy consumption is about 4.7 10^{20} J and is expected to grow at the rate of 2% each year for the next 25 years. Since the emergence of the apparition of the impending energy crises, various avenues are being explored to replace fossil fuels with renewable energy from solar power. In the past decades, the development of advanced molecular materials and nanotechnology, solar cells, and dye-sensitized solar cells, first of all, has initiated a new set of ideas that can dramatically improve energy conversion efficiency and reduce prices of alternative energy sources. Nevertheless, there are many fundamental problems to be solved in this area. Commercial competition of the new materials with existing fossil energy sources remains one of the most challenging problems for mankind.

This book embraces all principal aspects of structure and physicochemical action mechanisms of dye-sensitized collar cells (DSSCs) and photochemical systems of light energy conversion and related areas. A large body of literature exists on this subject and many scientists have made important contributions to this the field. The Internet program SkiFinder shows 44979 references for "dye sensitized" and 8493 references for "dye-sensitized collar cells." It is impossible in the space allowed in this book to give a representative set of references. The author apologizes to those he has not been able to include. More than 1000 references are given in the book, which should provide a key to essential relevant literature.

Chapter 1 of the monograph is a brief outline of the contemporary theories of electron transfer in donor–acceptor pairs and between a dye and a semiconductor. Principal stages of light energy conversion in biological photosystems, in which the Nature demonsrates excellent examples for solving problems of conversion of light energy to energy of chemical compounds, are described in Chapter 2. The light energy conversion in donor–acceptor pairs in solution and on templates is the subject of Chapter 3. Chapter 4 describes redox processes on the surface of semiconductors and metals. Chapters 1–4 form the theoretical and experimental background for the central Chapters 5 and 6. In Chapter 5, a general survey is made of fundamentals of the primary Gertzel dye-sensitized solar cell and its rapid development. Advantages in design of new type of dye-sensitized solar cells such as optical fiber, tandem, and solid-state DSSC and fabrication of its components are reviewed in Chapter 6. Chapter 7 gathers information on recent progress made in photocatalytic reduction and oxidation of water.

The monograph is intended for scientists and engineers working on dye-sensitized collar cells and other molecular systems of light energy conversion and related areas such as photochemistry and photosynthesis and its chemical mimicking. The book can be used as a subsidiary manual for instruction for graduate and undergraduate students of university chemistry, physics, and biophysics departments.

Gertz Likhtenshtein

1
Electron Transfer Theories

1.1
Introduction

Electron transfer (ET) is one of the most ubiquitous and fundamental phenomena in chemistry, physics, and biology [1–34]. Nonradiative and radiative ET are found to be a key elementary step in many important processes involving isolated molecules and supermolecules, ions and excess electrons in solution, condensed phase, surfaces and interfaces, electrochemical systems and biology, and in solar cells, in particular.

As a light microscopic particle, an electron easily tunnels through a potential barrier. Therefore, the process is governed by the general tunneling law formulated by Gamov [35]. The principal theoretical cornerstone for condensed phase ET was laid by Franck and Libby (1949–1952) who asserted that the Franck–Condon principle is applicable not only to the vertical radiative processes but also to nonradiative horizontal electron transfer. The next decisive step in the field was taken by Marcus and his colleagues [2, 17, 36] and Hash [37]. These authors articulated the need for readjustment of the coordination shells of reactants in self-exchange reactions and of the surrounding solvent to the electron transfer. They also showed that the electronic interaction of the reactants gives rise to the splitting at the intersection of the potential surfaces, which leads to a decrease in the energy barrier.

1.2
Theoretical Models

1.2.1
Basic Two States Models

1.2.1.1 Landau–Zener Model

The nonadiabatic electron transfer between donor (D) and acceptor (A) centers is treated by the Fermi's golden rule (FGR) [38]

Solar Energy Conversion. Chemical Aspects, First Edition. Gertz Likhtenshtein.

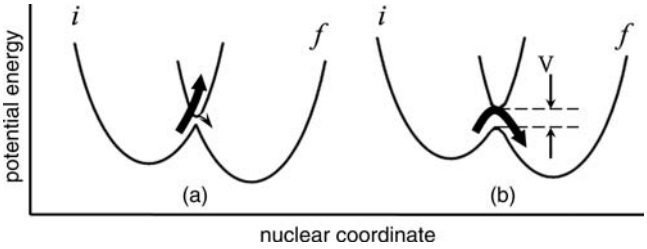

Figure 1.1 Variation in the energy of the system along the reaction coordinate: (a) diabatic terms of the reactant (i) and products (f); (b) adiabatic terms of the ground state (f) and excited state (f). V is the resonance integral [9].

$$k_{ET} = \frac{2\pi V^2 FC}{h} \tag{1.1}$$

where FC is the Franck–Condon factor related to the probability of reaching the terms crossing area for account of nuclear motion and V is an electronic coupling term (resonance integral) depending on the overlap of electronic wave functions in initial and final states of the process (see Figure 1.1).

At the transition of a system from one state to another, with a certain value of the coordinate Q_{tr}, the energy of the initial (i) and final (f) states of energy terms is the same and the law of energy conservation permits the term–term transition

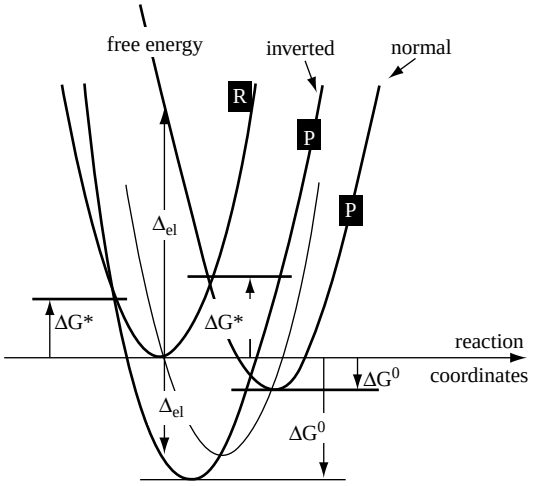

Figure 1.2 Energy versus reaction coordinates for the reactants and the products for normal and inverted reactions, and the inversion curve. The electron in the initial state requires a positive excitation energy Δel for the normal reaction and a negative excitation energy - Δel for the inverted reaction (which could be directly emitted as light). There is a positive energy barrier ΔF^* in both cases between the reactants and the products that requires thermal activation for the reaction to occur. This energy barrier as well as the energy for a direct electron excitation vanishes for the inversion curve and then the electron transfer becomes ultrafast. Reproduced from Ref. [61].

(Figure 1.2). Generally, the rate constant of the transition in the crossing area is dependent on the height of the energetic barrier (activation energy, E_a), the frequency of reaching of the crossing area (ψ), and the transition coefficient (κ):

$$k_{tr} = \kappa\nu \exp(-E_a) \tag{1.2}$$

The transition coefficient κ is related to the probability of the transition in the crossing area (P) and is described by the Landau–Zener equation [39, 40]:

$$\kappa = \frac{2P}{(1+P)} \tag{1.3}$$

where

$$P = 1 - \exp\left[\frac{-4\pi^2 V^2}{h\nu(S_i - S_f)}\right] \tag{1.4}$$

V is the electronic coupling factor (the resonance integral), ν is the velocity of nuclear motion, and S_i and S_f are the slopes of the initial and final terms in the Q_{tr} region. If the exponent of the exponential function is small, then

$$P = \frac{4\pi^2 V^2}{h\nu(S_i - S_f)} \tag{1.5}$$

and the process is nonadiabatic. Thus, the smaller the magnitude of the resonance integral V, the smaller is the probability of nonadiabatic transfer. The lower the velocity of nuclear motion and smaller the difference in the curvature of the terms, the smaller is the probability of nonadiabatic transfer. At $P = 1$, the process is adiabatic and treated by classical Arrhenius or Eyring equations.

The theory predicts a key role by electronic interaction, which is quantitatively characterized by the value of resonance integral V in forming energetic barrier. If this value is sufficiently high, the terms are split with a decreasing activation barrier and the process occurs adiabatically. In another nonadiabatic extreme, where the interaction in the region of the coordinate Q_{tr} is close to zero, the terms practically do not split, and the probability of transition i $\rightarrow$ f is very low.

1.2.1.2 **Marcus Model**

According to the Marcus model [2, 3, 5, 17, 36], the distortion of the reactants, products, and solvent from their equilibrium configuration is described by identical parabolas, shifted relative to each other according to the driving force of the value of the process, standard Gibbs free energy ΔG_0 (Figure 1.2). Within the adiabatic regime (strong electronic coupling, the resonance integral $V > 200\,cm^{-1}$), in the frame of the Eyring theory of the transition state, the value of the electron transfer rate constant is

$$k_{ET} = \left(\frac{h\nu}{k_B T}\right) \exp - \left[\frac{(\lambda + \Delta G_0)^2}{4\lambda k_B T}\right] \tag{1.6}$$

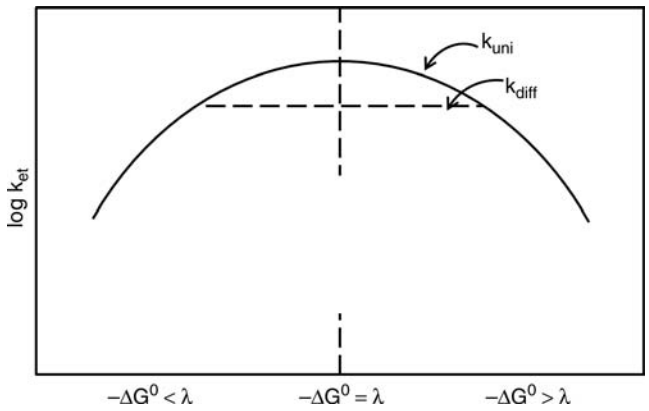

Figure 1.3 Variation in the logarithm of the rate constant of electron transfer with the driving force for the reaction after Marcus [50].

where λ is the reorganization energy defined as energy for the vertical electron transfer without replacement of the nuclear frame. Equation 1.6 predicts the log $k_{ET} - \Delta G_0$ relationships depending on the relative magnitudes of λ and ΔG_0 (Figure 1.3): (1) $\lambda > \Delta G_0$, when log k increases if ΔG_0 decreases (normal Marcus region); (2) $\lambda = \Delta G_0$, the reaction becomes barrierless; and (3) $\lambda < \Delta G_0$, when log k decreases with increasing driving force.

The basic Marcus equation is valid in following conditions:

1) All reactive nuclear modes, that is, local nuclear modes, solvent inertial polarization modes, and some other kinds of collective modes, are purely classical. The electronic transition in the ET process is via the minimum energy at the crossing of the initial and final state potential surfaces.
2) The potential surfaces are essentially diabatic surfaces with insignificant splitting at the crossing and of parabolic shape. The latter reflects harmonic molecular motion with equilibrium nuclear coordinate displacement and a linear environmental medium response.
3) The vibrational frequencies and the normal modes are the same in the initial and final states.

The Marcus theory also predicts the Brönsted slope magnitude in the normal Marcus region:

$$\alpha_B = \frac{d\Delta G^{\#}}{d\Delta G_0} = \frac{1}{2}\left(1 + \frac{\Delta G_0}{\lambda}\right) \tag{1.7}$$

The processes driving force (ΔG_0) can be measured experimentally or calculated theoretically. For example, when solvation after the process of producing photoinitiated charge pairing is rapid, ΔG_0 can be approximately estimated by the following equation:

$$\Delta G_0 = E_{D/D^+} - (E_{A/A^+} + E_{D^*}) - \frac{e^2}{\varepsilon}(r_{D^+} + r_{A^-}) \tag{1.8}$$

where E_{D/D^+} and $E_{A^+/A}$ are the standard redox potential of the donor and acceptor, respectively, E_{D^*} is the energy of the donor exited state, r_{D^+} and r_{A^-} are the radii of the donor and acceptor, respectively, and ε is the medium dielectric constant.

The values of λ can be roughly estimated within the framework of a simplified model suggesting electrostatic interactions of oxidized donor (D^+) and reduced acceptor (A^-) of radii r_{D^+} and r_{A^-} separated by the distance R_{DA} with media of dielectric constant e_0 and refraction index n:

$$\lambda = \frac{e^2}{2}\left(\frac{1}{n^2} - \frac{1}{e_0}\right)\left(\frac{1}{r_{D^+}} + \frac{1}{r_{A^-}} - \frac{2}{R_{DA}}\right) \tag{1.9}$$

1.2.1.3 Electronic and Nuclear Quantum Mechanical Effects

The nonadiabatic electron transfer between donor (D) and acceptor (A) centers is treated by the FGR (Equation 1.1). The theory of nonadiabatic electron transfer was developed by Levich, Dogonadze, and Kuznetsov [41–43]. These authors, utilizing the Landau–Zener theory for the intersection area crossing suggesting harmonic one-dimensional potential surface, proposed a formula for nonadiabatic ET energy:

$$k_{ET} = \frac{2\pi V^2}{h\sqrt{4\pi\lambda k_B T}} \exp\left[-\frac{(\lambda + \Delta G_0)^2}{4\lambda k_B T}\right] \tag{1.10}$$

Therefore, the maximum rate of ET at $\lambda = \Delta G_0$ is given by

$$k_{ET\,(max)} = \frac{2\pi V^2}{h\sqrt{4\pi\lambda k_B T}} \tag{1.11}$$

Involvement of intramolecular high-frequency vibrational modes in electron transfer was considered [44–49]. For example, when the high-frequency mode ($h\nu$) is in the low-temperature limit and solvent dynamic behavior can be treated classically [1], the rate constant for nonadiabatic ET in the case of parabolic terms is given by

$$k_{ET} = \frac{\sum_j 2\pi F_j V^2}{h\lambda k_B T} \exp\left[-\frac{(jh\nu + \lambda_s + \Delta G_0)^2}{4\lambda k_B T}\right] \tag{1.12}$$

where j is the number of high-frequency modes, $F_j = e^{-S}/j!$, $S = \lambda_v/h\psi$, and λ_v and λ_s denote the reorganization inside the molecule and solvent, respectively.

In the case of thermal excitation of the local molecular and medium high-frequency modes, theories mentioned before predicted the classical Marcus relation in the normal Marcus region. While in the inverted region, significant deviation on the parabolic energy gap dependence is expected (Figure 1.4). The inverted Marcus region cannot be experimentally observed if the stabilization of the first electron transfer product for the accounting of the high-frequency vibrational mode occurs faster than the equilibrium of the solvent polarization with the momentary charge distribution can be established. Another source of the deviation is the nonparabolic shape of the activation barrier [1].

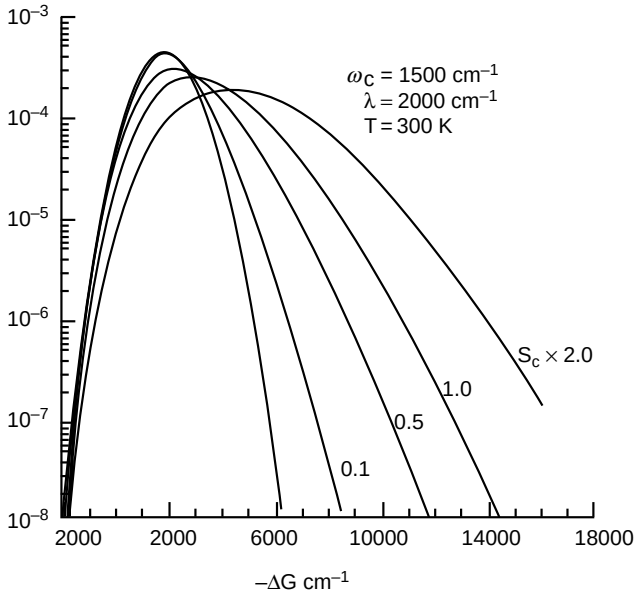

Figure 1.4 The energy gap dependence of the nuclear Franck–Condon factor, which incorporates the role of the high-frequency intramolecular modes. $S_c = \Delta/2$ is the dimensionless electron–vibration coupling, given in terms that reduce replacement (Δ) between the minimum of the nuclear potential surfaces of the initial and final electronic states [1]. Reproduced with permission.

A nonthermal electron transfer assisted by an intramolecular high-frequency vibrational mode has been theoretically investigated [18]. An analytical expression for the nonthermal transition probability in the framework of the stochastic point transition approach has been derived. For the strong electron transfer, the decay of the product state can vastly enhance the nonthermal transition probability in the whole range of parameters except for the areas where the probability is already close to unity. If the initial ion state is formed either by forward electron transfer or by photoexcitation, it may be visualized as a wave packet placed on the ion free energy term above the ion and the ground-state terms intersection (see Figure 6.1).

The Marcus inverted region cannot be observed experimentally when term-to-term transition in the crossing region is not a limiting step of the process as a whole (Figure 1.3) [50]. When ET reaction is very fast in the region of maximum rate, the process can be controlled by diffusion and, therefore, is not dependent on λ, V^2, and ΔG_0. The integral encounter theory (IET) has been extended to the reactions limited by diffusion along the reaction coordinate to the level crossing points where either thermal or hot electron transfer occurs [18]. IET described the bimolecular ionization of the instantaneously excited electron donor D^* followed by the hot geminate backward transfer that precedes the ion pair equilibration

$$D^* + A \underset{w_{21}}{\overset{w_{12}}{\longleftrightarrow}} [D^+ \quad \cdots \quad A^-] \xrightarrow{\bar{\varphi}} D^+ + A^-$$
$$w_{32} \updownarrow w_{23}$$
$$DA$$

and its subsequent thermal recombination tunneling is strong. It was demonstrated that the fraction of ion pairs that avoids the hot recombination is much smaller than their initial number when the electron tunneling is strong. The kinetics of recombination/dissociation of photogenerated radical pairs (RPs) was described with a generalized model (GM), which combines exponential models (EMs) and contact models (CMs) of cage effect dynamics [31]. Kinetics of nonthermal electron transfer controlled by the dynamical solvent effect was discussed in Ref. [11]. Recombination of ion pairs created by photoexcitation of viologen complexes is studied by a theory accounting for diffusion along the reaction coordinate to the crossing points of the electronic terms. The kinetics of recombination convoluted with the instrument response function were shown to differ qualitatively from the simplest exponential decay in both the normal and the inverted Marcus regions. The deviations of the exponentiality are minimal only in the case of activationless recombination and are reduced even more by taking into consideration a single quantum mode assisting the electron transfer

1.2.2
Further Developments in the Marcus Model

1.2.2.1 Electron Coupling

Variational transition-state theory was used to compute the rate of nonadiabatic electron transfer for a model of two sets of shifted harmonic oscillators [51]. The relationship to the standard generalized Langevin equation model of electron transfer was established and provided a framework for the application of variational transition-state theory in simulation of electron transfer in a microscopic (nonlinear) bath. A self-consistent interpretation based on a hybrid theoretical analysis that includes *ab initio* quantum calculations of electronic couplings, molecular dynamics simulations of molecular geometries, and Poisson–Boltzmann computations of reorganization energies was offered [52]. The analysis allowed to estimate the following parameters of systems under investigation: (1) reorganization energies, (2) electronic couplings, (3) access to multiple conformations differing both in reorganization energy and in electronic coupling, and (4) donor–acceptor coupling dependence on tunneling energy, associated with destructively interfering electron and hole-mediated coupling pathways. Fundamental arguments and detailed computations show that the influence of donor spin state on long-range electronic interactions is relatively weak.

The capability of multilevel Redfield theory to describe ultrafast photoinduced electron transfer reactions and the self-consistent hybrid method was investigated [53]. Adopting a standard model of photoinduced electron transfer in a condensed phase environment, the authors considered electron transfer reactions in the normal and inverted regimes, as well as for different values of the electron transfer parameters, such as reorganization energy, electronic coupling, and temperature.

A semiclassical theory of electron transfer reactions in Condon approximation and beyond was developed in [54]. The effect of the modulation of the electronic wave functions by configurational fluctuations of the molecular environment on the kinetic parameters of electron transfer reactions was discussed. A new formula for the transition probability of nonadiabatic electron transfer reactions was obtained and regular method for the calculation of non-Condon corrections was suggested. Quantum Kramers-like theory of the electron transfer rate from weak-to-strong electronic coupling regions using Zhu–Nakamura nonadiabatic transition formulas was developed to treat the coupled electronic and nuclear quantum tunneling probability [55]. The quantum Kramers theory to electron transfer rate constants was generalized. The application in the strongly condensed phase manifested that the approach correctly bridges the gap between the nonadiabatic (Fermi's golden rule) and adiabatic (Kramers theory) limits in a unified way, and leads to good agreement with the quantum path integral data at low temperature.

In work [56], electron transfer coupling elements were extracted from constrained density functional theory (CDFT). This method made use of the CDFT energies and the Kohn–Sham wave functions for the diabatic states. A method of calculation of transfer integrals between molecular sites, which exploits few quantities derived from density functional theory electronic structure computations and does not require the knowledge of the exact transition state coordinate, was conceived and implemented [57]. The method used a complete multielectron scheme, thus including electronic relaxation effects. The computed electronic couplings can then be combined with estimations of the reorganization energy to evaluate electron transfer rates. On the basis of the generalized nonadiabatic transition-state theory [58], the authors of the work [59, 60] presented a new formula for electron transfer rate, which can cover the whole range from adiabatic to nonadiabatic regime in the absence of solvent dynamics control. The rate was expressed as a product of the Marcus theory and a coefficient that represents the effects of nonadiabatic transition at the crossing seam surface. The numerical comparisons were performed with different approaches and the present approach showed an agreement with the quantum mechanical numerical solutions from weak to strong electronic coupling.

A nonadiabatic theory for electron transfer and application to ultrafast catalytic reactions has been discussed in Ref. [61]. The author proposed a general formalism that not only extends those used for the standard theory of electron transfer but also becomes equivalent to it far from the inversion point. In the vicinity of the inversion point when the energy barrier for ET is small, the electronic frequencies become of the order of the phonon frequencies and the process of electron tunneling is nonadiabatic because it is strongly coupled to the phonons. It was found that when the model parameters are fine-tuned, ET between donor and acceptor becomes reversible and this system is a coherent electron–phonon oscillator (CEPO). The acceptor that does not capture the electron may play the role of a catalyst (Figure 1.5). Thus, when the catalyst is fine-tuned with the donor in order to form a CEPO, it may trigger an irreversible and ultrafast electron transfer (UFET) at low temperature between the donor and an extra acceptor. Such a trimer system may be regulated by small perturbations and behaves as a molecular transistor.

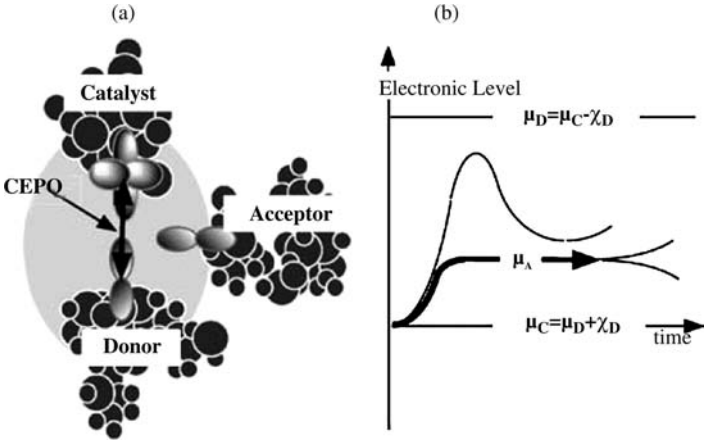

Figure 1.5 Principle of ET with a coherent electron–phonon oscillator [61].

Two weakly coupled molecular units of donor and catalyst generate a CEPO. This system is weakly coupled to a third unit, the acceptor (Figure 1.5a). An electron initially on the donor generates an oscillation of the electronic level of the CEPO. If the bare electronic level of a third molecular unit (acceptor) is included in the interval of variation, as soon as resonance between the CEPO and the acceptor is reached, ET is triggered irreversibly to the acceptor (Figure 1.5b). The authors suggested that because of their ability to produce UFET, the concept of CEPOs could be an essential paradigm for understanding the physics of the complex machinery of living systems.

Perturbation molecular orbital (PMO) theory was used to estimate the electronic matrix element in the semiclassical expression for the rate of nonadiabatic electron transfer at ion–molecular collisions [62]. It was shown that the electron transfer efficiency comes from the calculated ET rate divided by the maximum calculated ET rate and by dividing the observed reaction rate by the collision rate, calculated by the PMO treatment of ion–molecular collision rates.

1.2.2.2 **Driving Force and Reorganization Energy**

Several works were devoted to models for medium reorganization and donor–acceptor coupling [63–78]. The density functional theory based on *ab initio* molecular dynamics method combines electronic structure calculation and statistical mechanics and was used for first-principles computation of redox free energies at one-electron energy [66]. The authors showed that this is implemented in the framework of the Marcus theory of electron transfer, exploiting the separation in vertical ionization and reorganization contributions inherent in Marcus theory. Direct calculation of electron transfer parameters through constrained density functional theory was a subject of the work by Wu and Van Voorhis [67]. It was shown that constrained density functional theory can be used to access diabatic potential energy surfaces in the Marcus theory of electron transfer, thus providing a means to directly calculate the driving force and the inner sphere reorganization energy. The influence

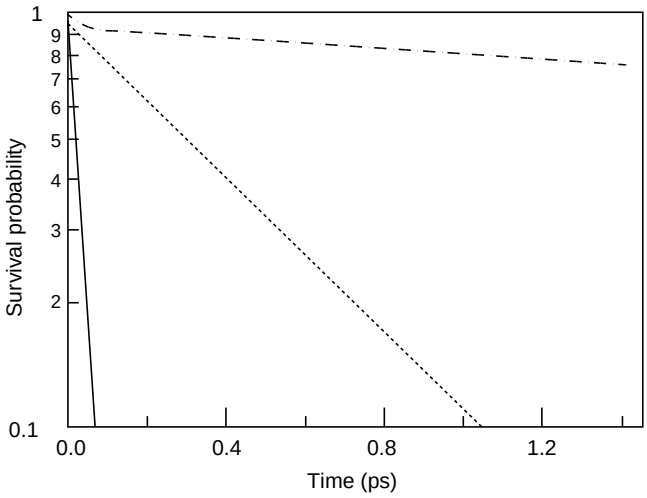

Figure 1.6 Survival probability as a function of time for D-B-A systems containing three (solid line), four (dotted line), and five (dashed line) subunits. All curves were calculated for the D-B-A system with the energy gap $\Delta\varepsilon$ between the donor and the equienergetic bridge equal to 1.2 eV. The value of the charge transfer integral V was taken to be equal to 0.3 eV [68].

of static and dynamic torsional disorder on the kinetics of charge transfer (CT) in donor–bridge–acceptor (D-B-A) systems has been investigated theoretically using a simple tight binding model [68]. Modeling of CT beyond the Condon approximation revealed two types of non-Condon (NC) effects. It was found that if τ_{rot} is much less than the characteristic time, τ_{CT}, of CT in the absence of disorder, the NC effect is static and can be characterized by rate constant for the charge arrival on the acceptor. For larger τ_{rot}, the NC effects become purely kinetic and the process of CT in the tunneling regime exhibits timescale invariance, the corresponding decay curves become dispersive, and the rate constant turns out to be time dependent. In the limit of very slow dynamic fluctuations, the NC effects in kinetics of CT were found to be very similar to the effects revealed for bridges with the static torsional disorder. The authors argued that experimental data reported in the literature for several D-B-A systems must be attributed to the multistep hopping mechanism of charge motion rather than to the mechanism of single-step tunneling. Survival probability as a function of time for D-B-A systems is shown in Figure 1.6.

The theory developed by Fletcher in Refs [71, 72] took into account the fact that charge fluctuations contribute to the activation of electron transfer, besides dielectric fluctuations. It was found that highly polar environments are able to catalyze the rates of thermally activated electron transfer processes because under certain well-defined conditions, they are able to stabilize the transient charges that develop on transition states. Plots of rate constant for electron transfer versus driving force are shown in Figure 1.7, which is drawn on the assumption that electron transfer is nonadiabatic and proceeds according to Dirac's time-dependent perturbation theory. On the

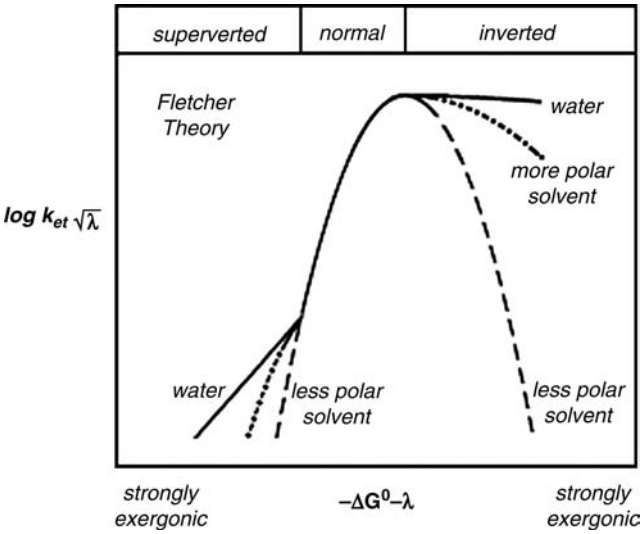

Figure 1.7 The rate constant for electron transfer (k_{ET}) as a function of the driving force ($-\Delta G^0$) and reorganization energy (λ) on the Fletcher theory [71, 72]. Note the powerful catalytic effect of polar solvents (such as water) on strongly exergonic reactions.

theory, the relative permittivity of the environment exerts a powerful influence on the reaction rate in the highly exergonic region (the "inverted" region) and in the highly endergonic region (the "superverted" region).

According to authors, nonadiabatic electron transfer is expected to be observed whenever there is small orbital overlap (weak coupling) between donor and acceptor states, so that overall electron transfer rates are slow compared to the media dynamics. For strongly exergonic electron transfer reactions that are activated by charge fluctuations in the environment, the activation energy was determined by the intersection point of thermodynamic potentials (Gibbs energies) of the reactants and products. The following equations for $G_{\text{reactants}}$ and G_{products}, which are the total Gibbs energies of the reactants and products (including their ionic atmospheres), respectively, were suggested:

$$G_{\text{reactants}} = \frac{1}{2} Q_1^2 \left(\frac{1}{4\pi\varepsilon_0}\right)\left(\frac{1}{\varepsilon(0)}\right)\left(\frac{1}{\alpha_D} + \frac{1}{\alpha_A} - \frac{2}{d}\right) \tag{1.13}$$

$$G_{\text{products}} = \frac{1}{2} Q_2^2 \left(\frac{1}{4\pi\varepsilon_0}\right)\left(\frac{1}{\varepsilon(\infty) + f_1\,[\varepsilon(0) - \varepsilon(\infty)]}\right)\left(\frac{1}{\alpha_D} + \frac{1}{\alpha_A} - \frac{2}{d}\right) \tag{1.14}$$

Q_1 and Q_2 are the charge fluctuations that build up on them, $\varepsilon(0)$ is the relative permittivity of the environment in the low-frequency limit (static dielectric constant), $\varepsilon(\infty)$ is the relative permittivity of the environment in the high-frequency limit ($\varepsilon \approx 2$), a_A is the radius of the acceptor in the transition state (including its ionic atmosphere), a_D is the radius of the electron donor in the transition state (including its ionic

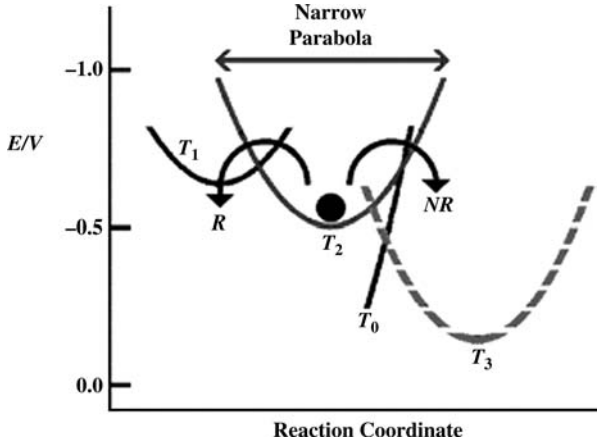

Figure 1.8 Superimposed Gibbs energy profiles in the vicinity of the electron trap T_2. Trapping is thermodynamically reversible, so the electron can return to T_0 radiatively (R) via T_1 or nonradiatively (NR) via the inverted region. Both routes are kinetically hindered by the extreme narrowness of the Gibbs energy parabola, however. This narrowness is conferred by the extremely nonpolar environment surrounding T_2. Trapping state T_3 is the final acceptor [72].

atmosphere), and f_1 is a constant $(0 < f_1 < 1)$ that quantifies the extent of polar screening by the environment, d is the distance between the electron donor and acceptor. Figure 1.8 shows the Gibbs energy for electron transfer through an intermediate.

Authors of paper [73] focused on the microscopic theory of intramolecular electron transfer rate. They examined whether or not and/or under what conditions the widely used Marcus-type equations are applicable to displaced–distorted (D-D) and displaced–distorted–rotated (D-D-R) harmonic oscillator (HO) cases. For this purpose, the cumulant expansion (CE) method was applied to derive the ET rate constants for these cases. In the CE method, the analytical condition was derived upon which the Marcus-type equation of the Gaussian form was obtained for the D-D HO case. In the frame of theory, the following equation for the ET rate constant was derived:

$$W_{b\to a} = \frac{|J_{ab}|^2}{\hbar^2}\sqrt{\frac{\pi\hbar^2}{\lambda k_B T}}\exp\left(-\frac{[\hbar\omega_{ab} + \langle V_{ab}(0)\rangle - \lambda + \lambda]^2}{4\lambda k_B T}\right) \tag{1.15}$$

where $\Delta G_{ab} = \hbar\omega_{ab} + \langle V_{ab}(0)\rangle - \lambda$ and $\hbar\omega_{ab} = E_a - E_b$.

The quantity $\hbar\omega_{ab} + \langle V_{ab}(0)\rangle$ has the following physical meaning. The quantity $\langle V_{ab}(0)\rangle$ is the vibrational energy acquired in the final state through vertical or FC transition from the initial state, averaged over the initial vibrational states under condition of vibrational thermal equilibrium in the initial potential energy surface.

It was found that the reorganization energy and the free energy change for the D-D HO depend on the temperature. As a consequence, the preexponential factor of the ET rate shows a temperature dependence different from the usual Arrhenius

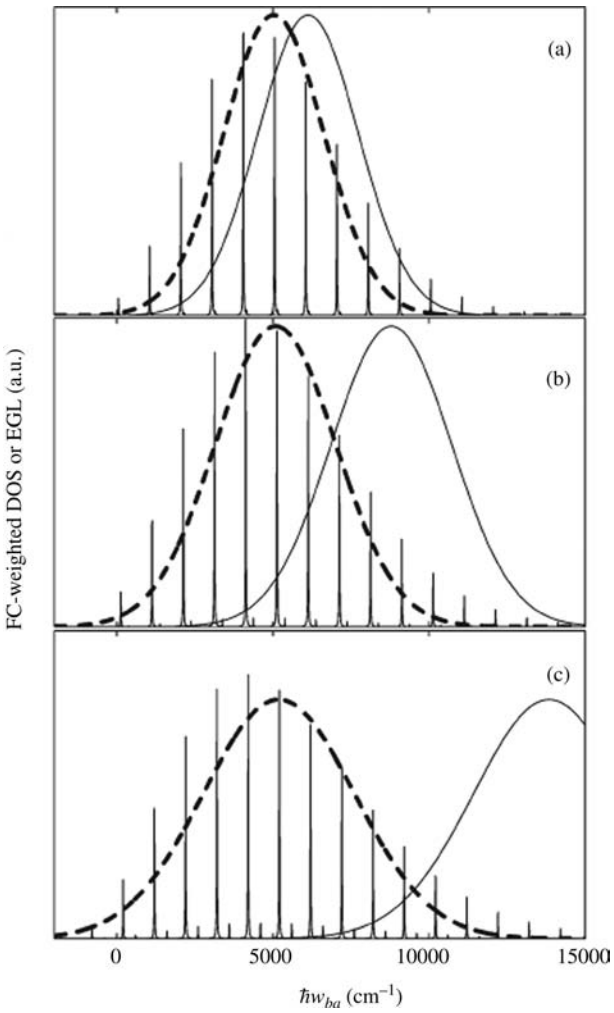

Figure 1.9 The dependent of the Franck–Condon weighted density 1 (FC DOS) (*y*-axis) on the degree of distortion for a model one-mode D-D HO system described in the text. The degrees of distortion are 0.9 in (a), 0.75 in (b), and 0.6 in (c). The peaks are the EGL calculated with the exact TCF method. The thick dashed lines denote the energy gap law (EGL) of the ET rate EGL calculated with the CE method using the same parameters. The thin smooth lines are the EGL calculated with the conventional Marcus theory [73].

behavior. The dependence of the Franck–Condon weighted density 1 on the degree of distortion for a model one-mode D-D HO system is presented in Figure 1.9.

The temperature dependence of the ET rate at different degrees of mixing for two modes whose frequencies are 100 and 30 cm^{-1} is shown in Figure 1.10.

The influence of spatial charge redistribution modeled by a change in the dipole moment of the reagent that experiences excitation on the dynamics of ultrafast

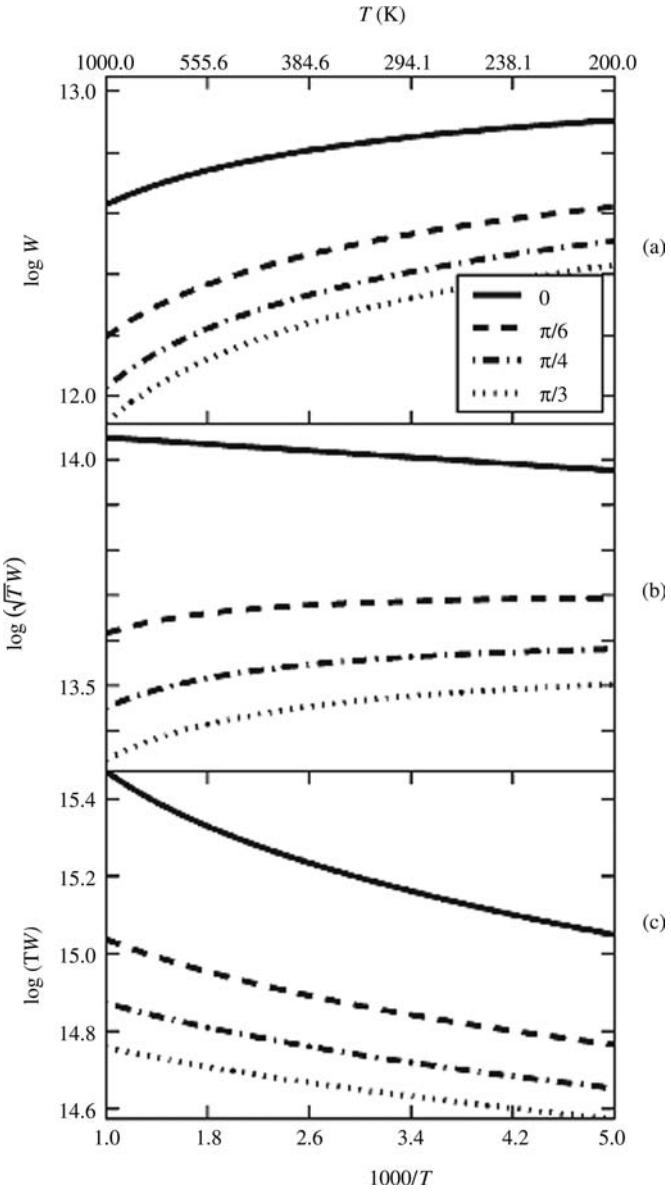

Figure 1.10 The temperature dependence of the ET rate at different degrees of mixing for two modes whose frequencies are 100 and 30 cm^{-1} in the lower level, without distortion. The abscissa is the inverse temperature, labeled in 1000/T. On the top, *T* (K) is also shown. (a) The ET rate on logarithmic scale versus the inverse temperature, for four different angles of rotation (labeled in the legend in radian). (b) The ET rate multiplied by the square root of the temperature, on logarithmic scale, versus the inverse temperature. (c) The ET rate multiplied by the temperature, on logarithmic scale, versus the inverse temperature [73].

photoinduced electron transfer was studied [22]. A two-center model based on the geometry of real molecules was suggested. The model described photoexcitation and subsequent electron transfer in a donor–acceptor pair. The rate of electron transfer was shown to depend substantially on the dipole moment of the donor at the photoexcitation stage and the direction of subsequent electron transfer. The authors of the work [74] have shown that the polarization fluctuation and the energy gap formulations of the reaction coordinate follow naturally from the Marcus theory of outer electron transfer. The Marcus formula modification or extension led to a quadratic dependence of the free energies of the reactant and product intermediates on the respective reaction coordinates. Both reaction coordinates are linearly related to the Lagrangian multiplier m in the Marcus theory of outer sphere electron transfer, so that m also plays the role of a natural reaction coordinate. When $m = 0$, $F^*(m = 0)$ is the equilibrium free energy of the reactant intermediate X^* at the bottom of its well, and when $m = -1$, $F(m = -1)$ is the corresponding equilibrium free energy of the product intermediate X. $Atm = -1$ the free energy of reorganization of the solvent from its equilibrium configuration at the bottom of the reactant. A theory of electron transfer with torsionally induced non-Condon (NC) effects was developed by Jang and Newton [69]. The starting point of the theory was a generalized spin-boson Hamiltonian, where an additional torsional oscillator bilinearly coupled to other bath modes causes a sinusoidal non-Condon modulation. Closed form time-dependent nonadiabatic rate expressions for both sudden and relaxed initial conditions, which are applicable for general spectral densities and energetic condition, were derived. Under the assumption that the torsional motion is not correlated with the polaronic shift of the bath, simple stationary limit rate expression was obtained. Model calculation of ET illustrated the effects of torsional quantization and gating on the driving force and temperature dependence of the electron transfer rate. The Born–Oppenheimer (BO) formulation of polar solvation is developed and implemented at the semiempirical (PM3) CI level, yielding estimation of ET coupling elements (V_0) for intramolecular ET in several families of radical ion systems [70]. The treatment yielded a self-consistent characterization of kinetic parameters in a two-dimensional solvent framework that includes an exchange coordinate. The dependence of V_0 on inertial solvent contributions and on donor–acceptor separation was discussed (see Figure 1.11).

In the work [76], it was demonstrated that constrained density functional theory allowed to compute the three key parameters entering the rate constant expression: the driving force (ΔG^0), the reorganization energy (λ), and the electronic coupling H_{DA}. The results confirm the intrinsic exponential behavior of the electronic coupling with the distance separating D and A or, within the pathway paradigm, between two bridging atoms along the pathway. Concerning the "through space" decay factors, the CDFT results suggested that a systematic parameterization of the various kinds of weak interactions encountered in biomolecules should be undertaken in order to refine the global "through space" decay factors. Such a work has been initiated in this paper. The hydrogen bond term has also been adjusted. Besides the refinement of the distance component, the authors underlined the appearance of an angular dependence and the correlation factor between R and ϕ.

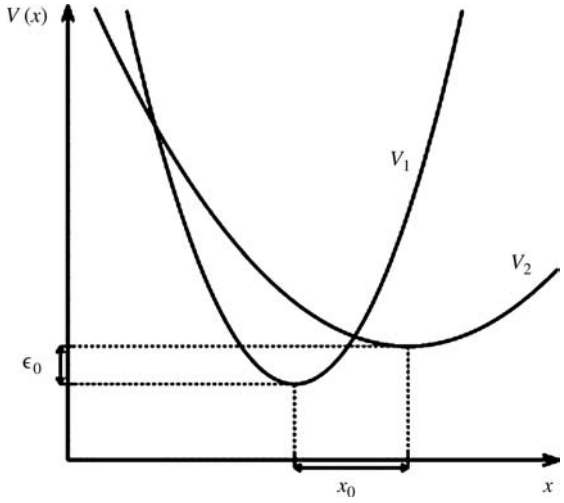

Figure 1.11 ET dynamics in a low temperature case for different reorganization energies (see details in Ref. [87, 88]).

Taking into account the volume of reagents, the theory gives the following Equation 1.16 [77]:

$$\lambda = \frac{e^2}{2}\left(\frac{1}{n^2} - \frac{1}{e_0}\right)\left(\frac{1}{r_{D^+}} + \frac{1}{r_{A^-}} - \frac{2}{R_{DA}} + \frac{\left[r_{D^+}^3 + r_{A^-}^3\right]}{2R_{DA}^4}\right) \tag{1.16}$$

Further development of theory of reorganization energy consisted in taking into consideration the properties of medium and manner in which it interfaces with the solute [65]. These properties must include both size and shape of the solute and solvent molecules, distribution of electron density in reagents and products, and the frequency domain appropriate to medium reorganization. When the symmetry of donor and acceptor is equivalent, reorganization energy can be generalized as

$$\lambda = C\Delta g_{\text{eff}}(e^2)\left(\frac{1}{r_{\text{eff}}} - \frac{1}{R_{DA}}\right) \tag{1.17}$$

where $C = 0.5$ is a coefficient, Δg_{eff} is the effective charge, and r_{eff} is the effective radius of charge separated centers. More general theory of the reorganization energy takes the difference between energies of the reactant state and product state, U_R and U_P, with the same nuclear coordinates q, as the reaction coordinate [78]:

$$\Delta e(q) = U_P(q) - U_R(q) \tag{1.18}$$

In this theory, the reorganization energy is related to the equilibrium mean square fluctuation of the reaction coordinate as

$$L = \frac{1}{2}(\beta < \Delta e - \langle \Delta e \rangle)^2 \tag{1.19}$$